Human Molecular Genetics, 2008, Vol. 17, No. 13 ***1968–1977***
doi:10.1093/hmg/ddn094
Advance Access published on March 25, 2008

A novel translation re-initiation mechanism for the *p63* gene revealed by amino-terminal truncating mutations in Rapp-Hodgkin/Hay-Wells-like syndromes

Tuula Rinne[1], Suzanne E. Clements[3], Evert Lamme[2], Pascal H.G. Duijf[4], Emine Bolat[1], Rowdy Meijer[1], Hans Scheffer[1], Elisabeth Rosser[5], Tiong Yang Tan[6], John A. McGrath[3], Joost Schalkwijk[2], Han G. Brunner[1], Huiqing Zhou[1] and Hans van Bokhoven[1,*]

[1]Department of Human Genetics and [2]Laboratory of Skin Biology and Experimental Dermatology, Radboud University Nijmegen Medical Centre, 6500 HB Nijmegen, The Netherlands, [3]St John's Institute of Dermatology, Division of Genetics and Molecular Medicine, The Guy's King's College and St Thomas' Hospitals' School of Medicine, London SE1 9RT, UK, [4]Department of Cancer Biology and Genetics, Memorial Sloan-Kettering Cancer Center, NY 10065, USA, [5]Department of Clinical Genetics, Great Ormond Street Hospital for Children, London WC1N 3EH, UK and [6]Genetic Health Services Victoria, Murdoch Children's Research Institute, Royal Children's Hospital, Victoria 3052, Australia

Received January 28, 2008; Revised and Accepted March 19, 2008

Missense mutations in the 3′ end of the *p63* gene are associated with either RHS (Rapp-Hodgkin syndrome) or AEC (Ankyloblepharon Ectodermal defects Cleft lip/palate) syndrome. These mutations give rise to mutant p63α protein isoforms with dominant effects towards their wild-type counterparts. Here we report four RHS/AEC-like patients with mutations (p.Gln9fsX23, p.Gln11X, p.Gln16X), that introduce premature termination codons in the N-terminal part of the p63 protein. These mutations appear to be incompatible with the current paradigms of dominant-negative/gain-of-function outcomes for other *p63* mutations. Moreover it is difficult to envisage how the remaining small N-terminal polypeptide contributes to a dominant disease mechanism. Primary keratinocytes from a patient containing the p.Gln11X mutation revealed a normal and aberrant p63-related protein that was just slightly smaller than the wild-type p63. We show that the smaller p63 protein is produced by translation re-initiation at the next downstream methionine, causing truncation of a non-canonical transactivation domain in the ΔN-specific isoforms. Interestingly, this new ΔΔNp63 isoform is also present in the wild-type keratinocytes albeit in small amounts compared with the p.Gln11X patient. These data establish that the p.Gln11X-mutation does not represent a null-allele leading to haploinsufficiency, but instead gives rise to a truncated ΔNp63 protein with dominant effects. Given the nature of other RHS/AEC-like syndrome mutations, we conclude that these mutations affect only the ΔNp63α isoform and that this disruption is fundamental to explaining the clinical characteristics of these particular ectodermal dysplasia syndromes.

INTRODUCTION

p53 Protein and its evolutionary predecessors p63 and p73 constitute a family of key transcriptional regulators in cell growth, differentiation and apoptosis. While *p53* is a major player in tumorigenesis, *p63* and *p73* appear to have pivotal roles in embryonic development. *p73*-Deficient mice have neurological and inflammatory problems, whereas

*To whom correspondence should be addressed at: Department of Human Genetics 588, Radboud University Nijmegen Medical Centre, PO Box 9101, 6500 HB Nijmegen, The Netherlands. Tel: +31 243616696; Fax: +31 243668752; Email: h.vanbokhoven@antrg.umcn.nl

p63-knockout mice have major defects in epithelial, limb and craniofacial development (1–3). These observations suggest that *p63* has a crucial role in tissue morphogenesis and maintenance of epithelial stem cell compartments. Furthermore, *p63* has been linked to several important signaling pathways, such as epidermal growth factor (EGF), fibroblast growth factor (FGF), bone morphogenetic protein (BMP), and Notch, Wnt (wingless-type) and Hedgehog (4–9).

The *p63* gene consists of 16 exons located on chromosome 3q28. At least six different protein isoforms can be produced, due to two different promoter sites and three different splicing routes. The amino-terminal ends are called TA and ΔN, and at the carboxy-terminal end, α, β and γ termini can be synthesized (Fig. 1). Several functional domains have been identified. The central DNA-binding domain and isomerization domain are present in all p63 isoforms. The canonical transcription activation (TA) domain is located at the amino-terminal end of the TAp63 isoforms. The ΔN-isoforms also contain an amino-terminal transactivation domain, denoted TA2 (10,11). The carboxy-terminal end has two additional domains: the sterile-alpha-motif (SAM) domain and a transactivation inhibitory (TI) domain, which are both only present in the largest carboxy-terminal variant, p63α (12).

Heterozygous mutations in the human *p63* gene cause developmental disorders, characterized by various combinations of ectodermal dysplasia (ED), limb malformations and orofacial clefting (13,14). To date, seven different disorders have been linked to mutations in the *p63* gene (15). These conditions may have overlapping phenotypic features, but some genotype–phenotype correlations have emerged (16). EEC syndrome (Ectrodactyly Ectodermal dysplasia and Cleft lip/palate, OMIM 604292) is the most common *p63*-linked ED. It is characterized by three major clinical symptoms: cleft lip and/or palate, ED (abnormal teeth, skin, hair, nails and sweat glands) and limb malformations in the form of split hand/foot (ectrodactyly) and/or fusion of fingers/toes (syndactyly). About 10% of *p63*-linked patients have Rapp-Hodgkin syndrome (RHS) (OMIM 129400) or AEC (Ankyloblepharon Ectodermal defects Cleft lip/palate)/Hay-Wells syndrome (OMIM 106260). These two latter syndromes fulfill the criteria of ED and orofacial clefting, but do not have the severe limb malformations seen in EEC syndrome. Some typical characteristics linked to RHS/AEC-like syndromes are eyelid fusion (ankyloblepharon filiforme adnatum), severe skin erosion at birth and abnormal hair with pili torti or pili canaliculi. Indeed, RHS and AEC syndromes are very similar and have been suggested to be variable manifestations of the same clinical entity (15,17). EEC and RHS/AEC syndromes are good examples of a strong genotype–phenotype association. Mutations in the EEC syndrome are clustered in the DNA binding domain, and most likely alter the DNA-binding properties of the protein. In contrast, mutations in RHS/AEC syndromes are clustered in SAM and TI domains in the carboxy-terminus of p63α (15–29). The SAM domain is involved in protein-protein interactions, whereas the TI-domain can bind intra-molecularly to the TA-domain, thereby inhibiting transcription activation (12,30). All *p63*-linked disorders are inherited in an autosomal dominant manner and mutations are thought to have either dominant-negative or gain-of-function effects (31).

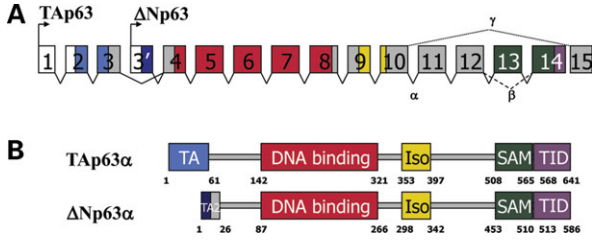

Figure 1. Schematic overview of the *p63* gene and two of its protein products. (**A**) *p63* has two different promoter sites resulting in two different N-terminal ends called TA and ΔNp63. ΔNp63 lacks the exons 1–3, which are present in TA, however it contains an alternative exon 3′. *p63* has three C-terminal splicing routes: α, β and γ, thus at least six different gene products can be transcribed. (**B**) The domain structure of TA and ΔNp63 is similar, only N-terminal transactivation domain is different, called TA and TA2, respectively. Domain abbreviations: ISO (isomerization domain), SAM (sterile-alpha-motif domain) and TID (transactivation inhibitory domain). The numbering under the domains illustrates the amino acid positions.

In this article we describe four patients from three families with phenotypes consistent with RHS/AEC syndromes that result from atypical nonsense mutations (p.Gln11X, p.Gln16X) or a deletion mutation (p.Gln9fsX23), all of which lead to a premature termination codon (PTC) in the early amino-terminal end of the ΔNp63-isoforms. These mutations are predicted to give rise to a null allele, which contradicts the accepted disease mechanism of other mutations. Surprisingly, in keratinocytes from the patient with the p.Gln11X mutation we were able to detect normal p63 RNA levels of both alleles, but also an additional smaller protein product. Using molecular studies we could demonstrate that the smaller p63 protein was produced by translational re-initiation at the next methionine after the PTC. This causes a deletion of 25 amino acids in the ΔNp63-isoforms, abrogating the TA2 domain, and thus suggesting a crucial role for this part of p63 in the pathogenesis of RHS/AEC syndromes.

RESULTS

Identification of atypical mutations predicting N-terminal premature stop codons

We identified four patients in three families with a clinical presentation reminiscent of AEC/RHS-like ED syndrome (for details see Materials and Methods). Direct sequencing of all 16 exons of the *p63* gene revealed three different heterozygous nucleotide changes in affected individuals. In family 1, both mother and daughter have a nucleotide change c.31C>T (Fig. 2A) (accession number AF075431) in the first coding exon, the alternative exon 3′, that is present only in the ΔNp63 isoform. The c.31C>T mutation changes glutamine to a stop codon at amino acid position 11, creating a PTC in all ΔNp63 isoforms. In family 3, a deletion of one nucleotide (c.26delA) was identified (Fig. 2B), also located in the alternative exon 3′ of ΔNp63 isoforms. This causes a frameshift and a PTC 41 nt downstream from the deletion (Fig. 2E). In family 2, a nucleotide change c.46C>T was detected in exon 4 (Fig. 2C). This mutation causes a change of glutamine to a stop codon at amino acid position 16 in the ΔNp63 isoforms and at position 71 in TAp63 isoforms. The genomic change

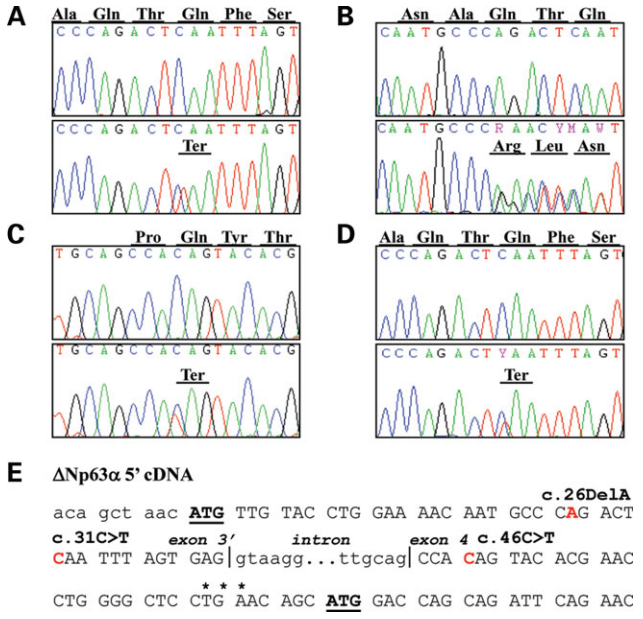

Figure 2. Pathogenic mutations in three RHS/AEC syndrome families. Direct sequencing of genomic DNA from four AEC/RHS patients revealed N-terminal mutations in the *p63* gene. (**A**) In family 1 a heterozygous nucleotide change c.31C>T was found in affected mother and daughter in exon 3′. The upper chromatogram illustrates a control sequence and the lower is from the affected mother. (**B**) In family 3, a heterozygous deletion c.26delA was detected in the index patient in exon 3′. The upper sequence is a control and the lower is from the patient. (**C**) In family 2 a heterozygous nucleotide change c.46C>T (ΔNp63-isoform) was detected in exon 4 in the index patient. The upper chromatogram illustrates a control DNA sequence and the lower is from the patient. (**D**) Chromatogram of the sequenced cDNA of keratinocytes from the mother of family 1 reveals the same heterozygous nucleotide change detected in the genomic DNA (Fig. 3A). Mutated RNA is present in the cells and is not degraded by the nonsense mediated RNA decay as expected. (**E**) The translated sequence of ΔNp63α (AF075431) (capitals) contains two AUG sites (bold, underlined) in the two first exons (exon 3′ and 4, | indicates the exon boundary). The mutated nucleotides: c.26A, c.31C and c.46C (indicated red and bold) are located between these two initiation sites. c.26delA mutation leads to a frameshift, which causes a PTC (indicated by ***) only 5 nt upstream of the second AUG site. c.31C>T changes the codon CAA into a termination codon TAA (this PTC is 44 nt upstream from the second AUG). c.46C>T changes codon CAG into a termination codon TAG causing a PTC 29 nt upstream of the second AUG. The second initiation codon is flanked by a strong Kozak sequence, where the most important nucleotides (purine at position −3 and a guanine at position +4) are conserved suggesting its use in translation re-initiation.

c.46C>T (or c.211C>T in TAp63 accession number AF075430) indicates a PTC in both ΔN and TAp63 isoforms. These three mutations were not identified in DNA from any of the unaffected family members nor in 300 control DNAs, indicating that they are all pathogenic, resulting in RHS/AEC-like syndromes.

Harmful and deleterious transcripts with a PTC are usually degraded through nonsense-mediated decay (NMD). In general, all transcripts containing a PTC upstream of the last exon junction complex are recognized and degraded (32). The c.31C>T mutation is present in the first exon of ΔNp63 followed by 11 exon junctions and c.26delA causes a PTC in the second exon (exon 4), followed by 10 exon junctions. c.46C>T (c.211C>T) causes a PTC in the second exon of ΔNp63 and in the fourth exon of TAp63, in both cases following 10 exon junctions. According to this paradigm, the transcripts with PTCs caused by these mutations should all be degraded by NMD and thereby cause *p63* haploinsufficiency.

To investigate this phenomenon in more detail we obtained a skin biopsy from the affected mother of family 1 and established a keratinocyte culture. p63 RNA expression levels in cultured keratinocytes were determined by quantitative PCR (qPCR) using two different primer sets specific for the 5′ end encoding ΔN-isoforms and one primer set for the 3′ end of the α-isoforms. All these three primer sets gave similar Ct-values suggesting that the major isoform in normal control keratinocytes is ΔNp63α (data not shown). Surprisingly, p63 RNA expression levels in cultured keratinocytes from the patient with the p.Gln11X mutation were similar to those of controls (Fig. 3), which refutes the *p63* haploinsufficiency model. We then sequenced the amplified RT-PCR products, which revealed that the nucleotide change c.31C>T was also present in the keratinocyte RNA pool. The presence of both alleles (Fig. 2D) argues against NMD.

N-terminal truncation of ΔNp63α due to translational re-initiation

Having established that the nonsense mutations do not have an effect on the mutant transcript levels, we next determined the consequences of the N-terminal mutations at the protein level. Western blot analysis performed on protein extracts from the patient's cultured keratinocytes with an antibody specific to the α-tail of p63, revealed an additional ΔNp63 protein of reduced molecular weight (3 kDa). A band of similar size was also present at very low levels in keratinocytes from control individuals, shown with the p63α-specific antibody in the western blot in Figure 4A. To resolve the identity of the smaller protein product, we investigated the nucleotide sequence downstream of the mutation. A further ATG codon was identified 44 nt downstream of the c.31C>T mutation (Fig. 2E). This is the first ATG codon following the canonical ΔN start codon and is located 75 nt downstream in the same reading frame. The Kozak sequence flanking this second AUG is in accordance with a strong translation initiation sequence, stronger even than the first AUG codon (Fig. 2E) (33,34). In addition, a translation start prediction program estimated this AUG to be an initiation site at score 0.631, a value within normal range of bonafide translation (Netstart 1.0 Prediction Server). We hypothesized that the next methionine downstream of the p.Gln11X mutation will be used to reinitiate the translation. A similar mechanism to escape NMD has been demonstrated previously for nonsense or frameshift mutations in *BRCA1*, *ATP7A* and *NEMO* genes (35–39).

To provide further support for the translation re-initiation hypothesis, we performed transfection studies in p63 negative Saos-2 cells. We performed transient transfections with a full-length ΔNp63α cDNA under a constitutive CMV promoter, pcDNA3_CMV_ΔNp63α. After transfections, the expression of each construct was confirmed by immunofluorescent labeling (data not shown). Protein lysate of each transfection was analyzed by western blotting. Firstly, we mutated the second methionine at position 26 to isoleucine to investigate whether this methionine is involved in translation initiation of the smaller ΔNp63α fragment. Wild-type ΔNp63α is

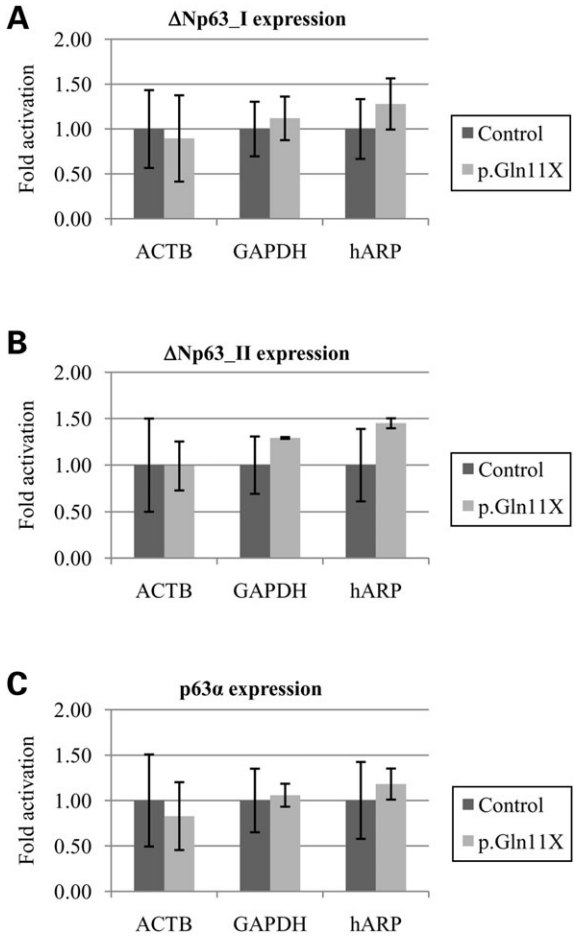

Figure 3. ΔNp63α levels in cultured keratinocytes from a Rapp-Hodgkin syndrome patient. ΔNp63 and p63α expression levels are investigated in undifferentiated keratinocytes by qPCR. The control (dark gray bar) is a pool of five control samples and the RHS patient sample (light gray bar) is from the mother of family 1 containing the p.Gln11X mutation. Housekeeping genes ACTB, GAPDH and hARP were used in normalization. qPCR with two ΔNp63 specific primer sets (**A** and **B**) show that ΔNp63 expression in RHS sample is very similar to the control, indicating that RNA containing the mutation is not degraded by NMD as expected. qPCR with p63α specific primer set gives similar results than ΔNp63 specific primer sets (**C**). Furthermore, similar Ct-values (data not shown) indicate ΔNp63α to be the only isoform expressed in undifferentiated cultured keratinocytes.

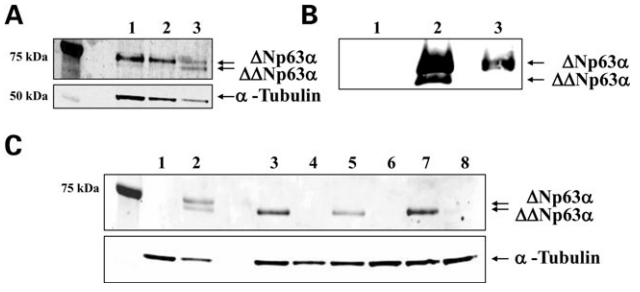

Figure 4. An additional ΔNp63α protein product in Rapp-Hodgkin syndrome patient is caused by translational re-initiation at methionine 26. (**A**) The lysate of cultured keratinocytes was run on NuPAGE®Bis–Tris Pre Cast Gels System. p63α-specific antibody H-129 [Santa Cruz] was used to detect the signal on nitrocellulose membrane. This experiment demonstrates two ΔNp63α protein variants in cultured keratinocytes. In control samples (lanes 1 and 2), the smaller ΔNp63α variant is present in small quantities. However, in the Rapp-Hodgkin syndrome sample (lane 3) the ratio is about one to one. α-tubulin [Abcam] is used as a loading control. (**B**) The second putative initiation site in ΔNp63, methionine 26, was mutated to isoleucine in a wild-type expression vector and transiently transfected into p63 negative Saos-2 cells, and harvested 30–48 h after transfection. The cell lysates were run on 8% SDS-Polyacrylamide gel and blotted to a nitrocellulose membrane. This was incubated with p63α-specific antibody H129 [Santa Cruz]. Mock (lane 1) is negative. When transfecting the wild-type ΔNp63α (lane 2) two p63 products are clearly present. However, when transfecting the mutation construct (Met26 is mutated into isoleucine), the lower product is missing (lane 3). This indicates that methionine at position 26 can initiate the translation. (**C**) N-terminal RHS and AEC mutations were also introduced to the expression vector along with the vector containing the Met26Ile mutation. These constructs were transfected into the Saos-2 cells and prepared as described above. Lane 1 contains empty vector pcDNA3. Wild-type ΔNp63α (lane 2) produces the double band similar to 4B. However, when transfecting the pathogenic mutations p.Gln11X (lane 3), p.Gln16X (lane 5) and p.Gln9fsX23 (lane 7) the upper product is completely absent. When a combination of pathogenic mutation plus a Met26Ile mutation is present [p.Gln11X_Met26Ile (lane 4), p.Gln16X_Met26Ile (lane 6) and p.Gln9fsX23_p.Met26Ile (lane 8)] no p63α protein product is detected at all. This experiment clearly demonstrates that all three pathogenic mutations cause translational re-initiation at methionine 26.

present in two protein bands, however, when methionine at position 26 is mutated, only the full-length ΔNp63α protein was present (Fig. 4B) and the smaller protein variant was undetectable, even upon high over-exposure of the blot. Secondly, all three pathogenic mutations (p.Gln11X, p.Gln16X and p.Gln9fsX23) and double mutants (p.Gln11X_Met26Ile, p.Gln16X_Met26Ile, p.Gln9fsX23_Met26Ile) were introduced into the ΔNp63α constructs. The transfection studies demonstrated a molecular size reduction (∼3 kDa) after introduction of the p.Gln11X, p.Gln16X or p.Gln9fsX23 mutation into cells (Fig. 4C), which is accordance with the additional protein observed in the patient's keratinocytes (Fig. 4A). Finally, when introducing the double mutant p.Met26Ile in combination with each pathogenic mutation, none of the two protein variants were detected (Fig. 4C). This strongly suggests that methionine 26 is used to initiate the translation of ΔΔNp63α in the presence of mutations that cause upstream premature stop codons. The shorter protein variant ΔΔNp63α was also detected in cells transfected with wild-type ΔNp63α, but at lower levels than the full-length protein. This phenomenon is similar to keratinocytes from control individuals, although the shorter variant is present in much lower levels compared with transfected cells.

Transcriptionally inactive ΔΔNp63α

The protein analysis showed that the p.Gln11X mutation causes an amino-terminal deletion of 25 amino acids. To study the transactivational activity of the ΔNp63 amino-terminus, we tested a series of truncation mutations in the ΔNp63γ isoform (Δ14, Δ26, Δ43, Δ61, Δ79) for transactivation activity (Fig. 5A). Full-length ΔNp63γ was able to activate an optimized p53 promoter nearly 6-fold more than the empty vector. In contrast, truncation of the first 14 amino acids completely abolished the activation (Fig. 5B). The same inactivating effect was detected for all other truncation mutations. Thus, 14 unique amino acids at the ΔN-terminus of p63 constitute a functional domain, which has transactivational

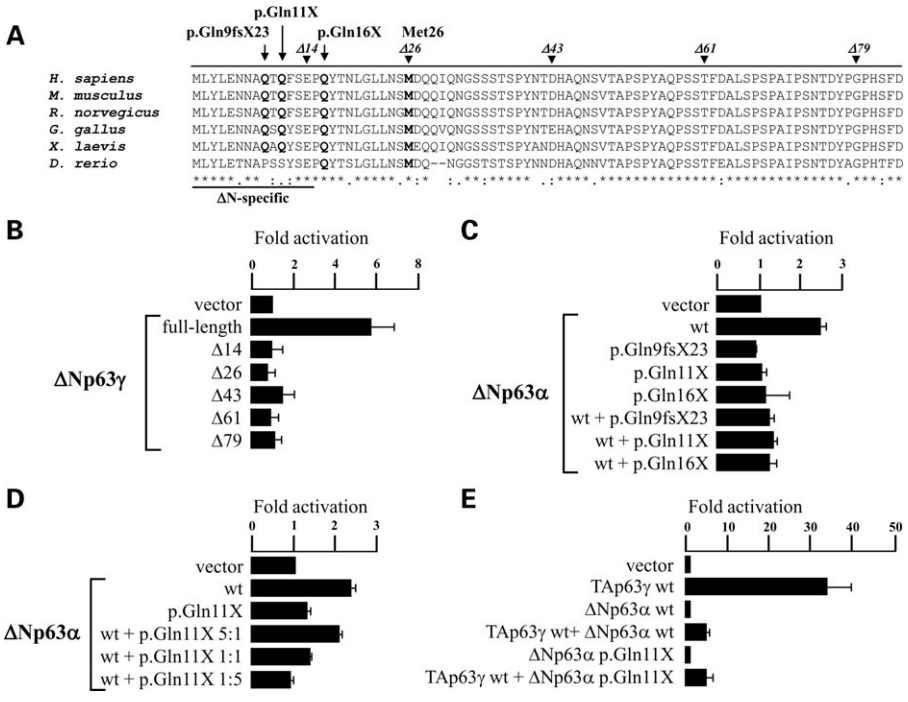

Figure 5. Transactivational activity in the N-terminus of ΔNp63 isoform. (**A**) Multiple sequence alignment represents the conservation of N-terminus of ΔNp63: all three glutamines mutated in RHS/AEC patients and the putative second translational initiation codon Met26 are almost fully conserved. The N-terminal truncation mutations are also indicated in this alignment. (**B**) Saos-2 cells were transiently transfected with N-terminally truncated p63 cDNA expression vectors (shown in Fig. 5A) and p53 promoter activation was measured. The truncated proteins lack the N-terminal 14 amino acids (Δ14, i.e. the residues which are unique for ΔNp63 isoforms) or N-terminal 26, 43, 61 or 79 amino acids (Δ26, Δ43, Δ61, Δ79, respectively). Full-length ΔNp63γ can activate the p53 promoter ∼6-fold, whereas deleting the first 14, 26, 43, 61 or 79 amino acids abrogates the transactivational activity completely. (**C**) Saos-2 cells were transfected with empty vector (pcDNA3), ΔNp63α wild-type, ΔNp63α mutant (p.Gln9fsX23, p.Gln11X and p.Gln16X) or combination of wild-type and mutant, and K14 promoter activation was then measured. The wild-type ΔNp63α is able to activate the K14 promoter 2.5 times, whereas none of the ΔNp63α mutants is able to activate the promoter at all. Neither co-transfection of wild-type and mutant are able to activate K14 promoter, indicating a dominant negative effect for the mutants. (**D**) Saos-2 cells were transfected with wild-type and p.Gln11X ΔNp63α constructs in different ratios and K14 promoter activity was measured. 5:1 ratio of ΔNp63α wild-type and p.Gln11X can activate K14 promoter similar to ΔNp63α wild-type construct, however, when using 1:1 or 1:5 ratio, which mimics RHS patient situation the activation is repressed and is similar to p.Gln11X construct. This supports the hypothesis that ΔΔNp63α is a dose-dependent regulator of ΔNp63α. (**E**) Finally, Saos-2 cells were transfected with TAp63γ and ΔNp63α isoforms. Wild-type TAp63γ can activate the p53-promoter 34 times when comparing with empty vector, whereas ΔNp63α cannot activate the promoter at all. Instead, ΔNp63α wild-type inhibits the activity of TAp63γ in a co-transfection assay. This dominant negative effect against the TAp63γ is also detected in the RHS p.Gln11X ΔNp63α, indicating that the mutated molecule is able to bind to the promoter.

activity. This is in accordance with previous studies on other promoters (10,11,40).

Because ΔNp63α is the predominant isoform in keratinocytes, we set out to test the ability of the p.Gln9fsX23, p.Gln11X and p.Gln16X mutants to regulate downstream target genes. Keratin-14 (K14) was recently reported to be a natural target gene of p63, which is upregulated by ΔNp63α (40–42). A transactivation assay of p63-negative Saos-2 cells transfected with either ΔNp63α wild-type, mutant or a combination of these constructs, together with a K14-luciferase-reporter construct, revealed that wild-type ΔNp63α was able to activate the K14 promoter 2.5 times more than the empty vector. This is in contrast to all ΔNp63α mutant constructs (p.Gln9fsX23, p.Gln11X and p.Gln16X), which were inactive and behaved similar to empty vectors (Fig. 5C). Co-transfections of each single mutation in combination with ΔNp63α wild-type vector showed no increased K14-promoter activation (Fig. 5C), indicating a dominant effect of these mutations against the wild-type. Next we investigated whether the mechanism of action of the mutant ΔNp63α protein might be dose dependent. To that end, we co-transfected Saos-2 cells with the wild-type and mutant constructs in a 5:1, 1:1 and 1:5 ratio (Fig. 5D). The 5:1 ratio of wild-type and p.Gln11X mutant was able to activate the K14-promoter 2.3-fold, which is similar to the wild-type ΔNp63α activation. In contrast, when we increased the amount of mutant p.Gln11X construct the activation was reduced to 1.2 and 0.8 in 1:1 and 1:5 ratios, respectively, indicating a dose-dependent inhibitory activity. Finally, we tested the dominant effect of mutant ΔNp63α_Gln11X towards TAp63γ isoform (Fig. 5E). ΔNp63α wild-type can inhibit the TAp63γ activation from ∼35-fold to 5-fold when compared with empty vector. The mutated ΔNp63α_Gln11X has a similar inhibitory activity as the wild-type ΔNp63α, indicating that the mutated protein can bind to DNA. These results show that mutant ΔNp63α isoforms have dominant effects towards various wild-type p63 isoforms and that they are dose-dependent.

DISCUSSION

Until now, mutations causing RHS and AEC syndrome have only been described in exons 13 and 14, which encode the SAM and TI domains of the p63α-protein. Here we report three RHS/AEC families without any changes in these exons, but with novel pathogenic mutations in the amino-terminus of ΔNp63: p.Gln9fsX23 and p.Gln11X (in the alternative exon 3′) and p.Gln16X (in exon 4). The first two are present in only the ΔNp63 isoforms, whereas the latter is present in both ΔNp63 and TAp63 isoforms. All these mutations lead to PTCs soon after the first translation initiation codon. Despite this, these mutant alleles still produce a p63-related protein by re-initiation of translation at the next ATG codon. Recently, similar translation re-initiation processes have been reported in genes causing other human inherited diseases, such as breast cancer, Menkes disease and Incontinentia pigmenti (36–39). Nevertheless, this is the first time that altered N-terminus and translation re-initiation has been linked to *p63* and RHS/AEC syndromes.

The mutations reported here are not associated with severe skin phenotype. Absence of skin defects is also observed in 60% RHS and 20% of AEC syndrome patients (28). Since we have studied only four patients, it cannot be concluded whether the lack of severe skin defects is related to the position of the mutations or just a reflection of the normal clinical variety in RHS/AEC. The three novel mutations we have reported are of particular interest, as they differ completely from the previously identified mutations in Rapp-Hodgkin and AEC syndromes. The 23 pathogenic mutations reported so far in *p63* in these disorders are missense mutations, deletions or insertions clustered in the α-terminus of p63, changing the composition of the SAM and TI domains (15–29). However, our new findings, based on the sites of the p.Gln11X, p.Gln16X and p.Gln9fsX23 mutations, imply that ΔNp63α is the critical isoform causing RHS/AEC syndrome. One of the new mutations we report (p.Gln16X/p.Gln71X) also affects the TA-isoform, although since ΔNp63α is the only p63 isoform (>99%) expressed in epithelial tissues, the relevance of TA-isoform disruption remains obscure (8,40). Moreover, the phenotype of the patient carrying the p.Gln16X/p.Gln71X mutation is not significantly different from that of the patients with the other mutations in families 1 and 3. This strongly indicates that either an aberrant ΔN- or α-terminus of p63 cause a condition which is characterized by ED and orofacial clefting, but not developmental limb problems.

It has been shown previously that ΔNp63α can function both as an activator and a repressor of transcription (10,40,43–45). We tested transactivational activity of p.Gln9fsX23, p.Gln11X and p.Gln16X in a transactivation assay on the K14 promoter, on which ΔNp63α acts as an activator of transcription. Mutant constructs are unable to activate the K14 promoter (Fig. 5C), indicating that the first 25 amino acids are crucial for the activation. This is in accordance with the results of transactivation assays in this paper (Fig. 5B), in which deletion mutants affect the N-terminal TA2 domain. In addition, in previous assays the N-terminal deletion abrogates the activity to transactivate p53 target genes and induce cell cycle arrest and apoptosis (10,11). Our TAp63γ co-transfection assay show that the p.Gln11X mutant can inhibit TAp63γ-mediated transactivation (Fig. 5E), indicating that this mutant is able to bind to DNA and form heteromers with other p63 isoforms. Previously, we have demonstrated that the SAM domain mutant proteins have lost their ability to form p63-protein complexes and their ability to bind to DNA (18). Apparently, the ΔN-mutant proteins have retained these properties. It is unclear whether these properties have an effect on the phenotype since they are highly similar, except perhaps for the skin phenotype, which is not severe in the patients with N-terminal mutation. In addition, the ΔNp63α co-transfection assay shows that all these three mutants can inhibit ΔNp63α wild-type transactivation (Fig. 5C), suggesting that these mutations have a dominant negative effect.

The first 25 amino acids in the ΔNp63α are crucial for the correct function of the ΔNp63-isoforms. The shorter ΔΔNp63α variant was also detected in wild-type keratinocytes as well as in ΔNp63α-transfected Saos-2 cells (Fig. 4). In keratinocytes, this new isoform appears to be more abundant than any other p63 isoform (TA, β, γ) except ΔNp63α. This indicates that the *p63* gene encodes more protein isoforms than the six that have been recognized to date (Fig. 1). Therefore, this p63 variant appears to be a novel translational variant and apparently not deleterious for the cells. We hypothesize that in keratinocytes the ΔΔNp63α isoform has a regulatory function, which is imbalanced in patients because of the increased amount of ΔΔNp63α. Our dose-dependent assay of ΔNp63α and ΔΔNp63α on K14 promoter also showed that elevated amount of ΔΔNp63α represses the ΔNp63α activation (Fig. 5D). Thus, the disturbed ratio between the full-length and shorter p63 variant might be relevant for causing the disease phenotype. Since AEC/RHS is a dominantly inherited disease, we propose a dominant-negative effect of the ΔΔN-isoform against wild-type ΔN-isoform in either a dimer or tetramer structure. Once the mutated and wild-type isoform form a functional protein complex, the ΔΔN-isoform may alter the function of this complex, working as a repressor or an activator.

Both ΔN- and α-terminal mutations can lead to a highly similar clinical phenotype, although the molecular mechanisms involved in the pathogenesis are as yet unknown. The TI-domain of the α-terminus intra-molecularly binds to the N-terminal TA-domain, even though this has not been reported for the ΔN-terminus of ΔNp63α (12). It appears however, that both types of mutations have an effect on transcription regulation by ΔNp63α. Here we have shown that deletions of ΔNp63 result in reduced transactivation activity by ΔNp63α on p53 and p63 promoters. Previously we have shown that SAM-domain mutants ablate the transactivational inhibitory effects of ΔNp63α towards transactivation by p53 and TAp63γ (18). Consequently, both N-terminal and SAM-domain mutations associated with RHS/AEC syndrome appear to affect transactivation activity by ΔNp63α isoforms. A systematic screening of the effects of constructs with N- and C-terminal mutations on a panel of natural p63 target genes and in a relevant cell type, such as in keratinocytes, may give further insight into the precise disease mechanism in RHS/AEC syndrome. From the present study, we conclude that the generation of an N-terminally truncated ΔNp63α

protein is responsible for causing a Rapp-Hodgkin and AEC syndrome-like phenotype.

MATERIAL AND METHODS

Clinical study

The index patient of family 1 is a 6-year-old girl, who has a unilateral cleft lip and palate. She has coarse dry blond hair and fair skin and there is scaling on the forehead, around the nipples and on the buttocks. She is anhidrotic. At birth she had a systolic murmur, but on ultrasound was found to have a normal cardiac anatomy and the murmur appeared to be innocent. The index patient's mother also has ED: her hair has a coarse texture and a spiky appearance. Her skin is dry, and she has hypodontia of her primary teeth and her fingernails are dystrophic. She has anhidrosis on her trunk and limbs but is able to sweat normally from her palms and soles. In addition, she has had frequent urinary tract infections. Unlike her daughter she has secondary hearing loss due to a malformation of the external ear canal. She also had a history of a malignant melanoma, which had been excised from her right hand.

The index patient of family 2 is a 2-year-old boy, who was born to non-consanguineous parents of Greek-Australian descent. He has a unilateral cleft of the soft palate and left-sided ankyloblepharon filiforme. He has sparse eyebrows and eyelashes in infancy, but no alopecia or dry skin. He has small nails, which are not dystrophic. He also has hypoplastic alae nasi. There are no dental anomalies or delayed dental eruption.

The patient in family 3 is a 13-year-old girl. She was born with an absent hard palate in her mouth, ankyloblepharon filiforme and an atrial septal defect. As an infant she was prone to infections, but this later improved. She has upslanting palpebral fissures, a long nose and a small mouth with a thin upper lip. She has sparse eyelashes, but extremely thick and bushy hair, which is easy to brush. Her hands, feet and nails are all normal.

Mutation analysis

Blood samples and skin samples used in this study were obtained after written informed consent was obtained. Genomic DNA was extracted from peripheral blood samples by a standard salting-out method. All 16 exons of the *p63* gene were amplified and sequenced in both directions. Primers, which were used to amplify the alternative exon 3′ and exon 4 are illustrated in Table 1A.

Cell culture

A skin biopsy (4 mm diameter) was taken from the back of the index patient's mother. The skin was collected in RMPI [Gibco] medium with Gentamycin (1:1000) [Gibco], Amphotericin (1:100) [Gibco] and Penicillin/Streptomycin [Gibco]. The biopsy was then trypsinized in 0.25% Trypsin–PBS [Brunschwig] overnight at 4°C following which the upper epidermal layer was separated from the biopsy with tweezers and the dermal surface was scratched smoothly to release the keratinocytes. Serum was added to stop the trypsin activity. Next the solution containing the dermal and epidermal components was vortexed at low speed for 1 min. The dermal parts were removed and the epidermal cells were added on to irradiated 3T3-J2 cells. Cells were cultured in Green's medium: DMEM [Gibco], Ham's F12 [Gibco] (2:1) supplemented with 10% fetal bovine serum [Hyclone], 4 mM L-Glutamine [ICN Biomedicals], 100 U/ml penicillin [Gibco], 100 μg/ml streptomycin [Gibco], 25 μg/ml adenine [Calbiochem], 5 μg/ml insulin [Sigma], 0.4 μg/ml hydrocortisone [Calbiochem], 1.4 ng/ml triiodothyronine [Sigma], 0.1 nM Cholera toxin [Sigma]. EGF (10 ng/ml) [Sigma] was added to the medium 3 days after starting the keratinocyte culture. The medium was refreshed every second day until the culture reached 80–90% confluence. The primary keratinocyte stocks were stored in liquid nitrogen.

Mouse fibroblast cell line 3T3-J2 was used as a feeder layer for the keratinocytes in Green's medium. Pure 3T3-J2 cells were cultured in DMEM w/o pyruvate [Gibco] containing 10% calf serum supplemented by iron [Hyclone] and 100 U/ml penicillin [Gibco] and 100 μg/ml streptomycin [Gibco]. 3T3 cells were irradiated at 3500 cGy about 20 h before adding keratinocytes.

Keratinocytes were cultured at 37°C in 5% CO_2 in Keratinocyte growth medium (KGM). This medium consists of Keratinocyte Basal Medium, 0.15 mM Ca^{2+} [Cambrex], supplemented with 0.1 mM ethanolamine [Sigma], 0.1 mM phosphoethanolamine [Sigma], bovine pituitary extract (0.4%) [Bio Whittaker], 10 ng/ml EGF [Sigma], 5 μg/ml insulin [Sigma], 0.5 μg/ml hydrocortisone [Calbiochem], 100U/ml penicillin [Gibco] and 100 μg/ml streptomycin [Gibco]. The medium was changed every second day until the culture reached confluent state.

Transfection conditions

Human osteoblast cell line Saos-2 was used for transient transfections. Saos-2 cells were cultured in DMEM [Gibco] supplemented by 10% fetal calf serum [Sigma], 1% natrium-puruvate [Gibco], 1% Glutamax-1 [Gibco] and 100 U/ml penicillin [Gibco] and 100 μg/ml streptomycin [Gibco]. Approximately 1.5×10^5 Saos-2 cells were seeded in one well of a 6-well tissue culture plate. Effectene transfection reagent [Qiagen] was used to transfect the pcDNA3, pcDNA3_Mm_ΔNp63α (43) wild-type and its mutant versions p.Gln11X, p.Gln16X, p.Gln9fsX23, Met26Ile and double mutant p.Gln11X_Met26Ile, p.Gln16X_Met26Ile and p.Gln9fsX23_p.Met26Ile constructs into Saos-2 cells. The same method was used for co-transfections, where either pcDNA3_ΔNp63α wild-type was transfected together with each single mutant (p.Gln11X, p.Gln16X, p.Gln9fsX23) ΔNp63α construct or pcDNA3_TAp63γ wild-type was transfected together either with wild-type or mutant (p.Gln11X) pcDNA3_ΔNp63α construct. The cells were collected 30–48 h after transfection.

For transfections of the ΔNp63 truncation mutations (Δ14, Δ26, Δ43, Δ61, Δ79), Saos-2 cells were plated on 18 mm round glass coverslips and a total of 2 μg plasmid DNA was transfected using a calcium phosphate precipitation protocol (46).

Table 1. Oligonucleotide sequences

A	**GenBank number**	**Exon**	**Forward (5′>3′)**	**Reverse (5′>3′)**	**Primer for**
	NT_005612.15	*p63* Exon 3′	gcctcctcatgcctatagttg	tcttacagccaccacagaaaa	PCR, sequencing
	NT_005612.15	*p63* Exon 4	gatccgtggcttcagcgg	aagcccatccttggacttgg	PCR, sequencing
B	**GenBank number**		**Forward (5′>3′)**	**Reverse (5′>3′)**	
	AF_075431	ΔNp63	ctggaaaacaatgcccagac	gggtgatggagagagagcat	RT-PCR
C	**GenBank number**		**Forward (5′>3′)**	**Reverse (5′>3′)**	
	AF_075431	ΔNp63	caatgcccagactcaatttagtga	tgctggtccatgctgttcag	RT-qPCR
	AF_075431	ΔNp63	ttgtacctggaaaacaatgcc	tgctggtccatgctgttcag	RT-qPCR
	AF_075431	p63α	tccatggatgatctggcaagt	gcccttccagatcgcatgt	RT-qPCR
	NM_001101	ACTB	actggaacggtgaaggtgaca	agggacttcctgtaacaacgca	RT-qPCR
	NM_001002	hARP	caccattgaaatcctgagtgatgt	tgacaagcccaaaggagaag	RT-qPCR
	NM_002046	GAPDH	tgcaccaccaactgcttagc	ggcatggactgtggtcatgag	RT-qPCR
D	**Plasmid**		**Forward (5′>3′)**	**Reverse (5′>3′)**	
	pcDNA3_Mm_ΔNp63α	p.Gln11X (c.31C>T)	gaaaacaatgcccagacttaatttagtgagccacagt	actgtggctcactaaattaagtctgggcattgttttc	Mutagenesis
	pcDNA3_Mm_ΔNp63α	p.Gln16X (c.46C>T)	caatttagtgagccatagtacacgaacctgg	ccaggttcgtgtactatggctcactaaattg	Mutagenesis
	pcDNA3_Mm_ΔNp63α	p.Gln9Xfs23 (c.26delA)	ctggaaaacaatgcccgactcaatttagtgag	ctcactaaattgagtcgggcattgttttccag	Mutagenesis
	pcDNA3_Mm_ΔNp63α	p.Met26Ile (c.78G>A)	gctcctgaacagcatagaccagcagattcag	ctgaatctgctggtctatgctgttcaggagc	Mutagenesis
	pcDNA3_Mm_ΔNp63γ	Δ14	ccacagtacacgaacctggggctcc	catccgcggggcaggggtcccggaa	Mutagenesis
	pcDNA3_Mm_ΔNp63γ	Δ26	gaccagcagattcagaacggctcc	catccgcggggcaggggtcccggaa	Mutagenesis
	pcDNA3_Mm_ΔNp63γ	Δ43	cacgcacagaatagcgtgacggcgc	catccgcggggcaggggtcccggaa	Mutagenesis
	pcDNA3_Mm_ΔNp63γ	Δ61	tttgatgccctctctccatcccctg	catccgcggggcaggggtcccggaa	Mutagenesis
	pcDNA3_Mm_ΔNp63γ	Δ79	cacagcttcgatgtgtccttccagc	catccgcggggcaggggtcccggaa	Mutagenesis

Luciferase assays

Subconfluent Saos-2 cells were transfected as described above at a 1:2 ratio between the reporter construct (firefly luciferase under control of K14 promoter) (kind gift of Dr B. Andersen and Dr E. Candi) and the wild-type or mutant (p.Gln11X, p.Gln16X, p.Gln9fsX23) pcDNA3_ΔNp63α or a combination of wild-type and mutant vector. In addition, 50 ng of Renilla luciferase construct was co-transfected in each transfection to normalize for transfection efficiency. After 30 h the transfection luciferase activities were measured using a Dual Luciferase Reporter Assay System [Promega] according to the manufacturer's instructions. The level of activation was calculated in comparison with transfections with an empty pcDNA3 vector.

Transfections for the TAp63γ co-transfection assay were carried out as described above at a 1:3 ratio between the reporter construct (β-galactosidase reporter under p53 promoter) and expression construct (pcDNA3_Mm_TAp63γ wild-type, pcDNA3_ΔNp63α wild-type or p.Gln11X mutant construct, or in co-transfections TAp63γ in combination with ΔNp63α wt or mutant). In addition, 5 ng of Renilla luciferase construct was transfected in each transfection to normalize for transfection efficiency. After 30 h the transfection β-galactosidase and luciferase activities were measured using a Luminescent beta-galactosidase detection kit II [Clontech] and a Renilla Luciferase Reporter Assay System [Promega] according to the manufacturer's instructions. The level of activation was calculated in comparison with transfections with an empty pcDNA3 vector. Transactivation assays of the truncation mutations were carried out as described previously (43).

Mutagenesis

Pathogenic mutations of interest were introduced into the pcDNA3_ΔNp63α vector by using QuickChange Site-Directed Mutagenesis kit [Stratagene] according to the manufacturer's instructions. The p.Gln11X, p.Gln16X, p.Gln9fsX23 and p.Met26Ile mutations were introduced in this vector. The p.Gln11X, p.Gln16X and p.Gln9fsX23 mutations were also introduced into pcDNA3_ΔNp63α_Met26Ile mutation construct to create double mutations. Mutagenesis primers are shown in Table 1D. The correct sequence of each clone was determined by direct sequencing of the entire cDNA insert.

N-terminal deletion mutations were introduced into pcDNA3_Mm_ΔNp63γ vector by using ExSite PCR-based site-directed mutagenesis procedure [Stratagene] according to the manufacturer's instructions. The sequences encoding amino acids 2–14, 2–26, 2–43, 2–61 and 2–79 (amino acid numbers referring to ΔNp63 protein) were removed using oligonucleotides described in Table 1D. The obtained clones were screened for the presence of the respective deletions by direct sequencing using primers flanking the deletions.

Sample preparation and immunoblotting

Transfected Saos-2 cells and keratinocytes were harvested in PBS and centrifuged at 4°C at 3000 RPM for 10 min. The pellet was lysed in lysis buffer containing: 50 mM Tris-HCl pH 7.8, 10% glycerol [Invitrogen], 0.5% Nonidet-P40 [Brunschwig], and 5 mM Ethylene glycol-bis-tetraacetic acid (EGTA) [Fluka], and freshly added 10 mM β-mercaptoethanol [Sigma], 0.5 mM Phenylmethanesulfonyl fluoride [Fluka], 1 μg/ml Pepstatin A [Fluka] and 1× protease inhibitory cocktail [Roche], for 20 min on ice. Immunoblotting was performed using the NuPAGE®Bis-Tris Pre Cast Gel System [Invitrogen] following the manufacturer's instructions. Samples were run on a 4–12% NuPAGE®Bis-Tris gel in MOPS buffer [Invitrogen]. p63α-Specific polyclonal antibody H-129 (1:500) [Santa Gruz] was used to detect p63 and a mouse monoclonal α-Tubulin antibody DM1A (1:5000) [Abcam] was used as a loading control. Alexa-680 goat-anti-rabbit secondary antibody [Molecular Probes] and IrDye-800 goat-anti-mouse secondary antibody [Rockland]

were both used in 1:5000 dilution. The signal detection was performed by Odyssey scanner [Licor].

RNA isolation

Keratinocytes were cultured in KGM and harvested either at confluent state or after 48 h differentiation. Total RNA isolation was performed using the RNeasy mini kit [Qiagen] according the manufacturer's instructions. RNA was treated with DNase I while bound to the RNeasy column to remove residual traces of genomic DNA [Qiagen]. The integrity of the RNA was assessed on an agarose gel, and the concentration and purity were determined with a ND-1000 spectrophotometer [Nanodrop].

Reverse transcriptase PCR

Two μg of total RNA was transcribed into cDNA as described earlier (47). cDNA was amplified with a forward primer specific to alternative exon 3′ of *p63* gene and a reverse primer specific to exon 4 with a total number of 35 cycles. Primer sequences are in Table 1B. The RT-PCR product was electrophoresed in an agarose gel and purified using the Qiaquick gel extraction kit [Qiagen]. This cDNA product was sequenced with reverse primer by using a 3730 DNA analyzer from Applied Biosystems.

Quantitative PCR

qPCR was performed on the iQ-apparatus [MyiQ single-color real-time detection system (Biorad)] by using iQ SYBR® Green Supermix [Biorad] according to the manufacturer's protocol. All primer pairs were designed such that they cover either separate exons or that one is spanning an exon-exon boundary. All primers were validated in triplicate by use of serial cDNA dilutions, and were confirmed for 100 ± 5% efficiency. Differences in the expression of a gene of interest between two samples were calculated by $2^{\Delta\Delta Ct}$ method (48,49). To normalize the amount of cDNA we used three housekeeping genes: beta-actin (ACTB), hARP (human acidic ribosomal protein) and GAPDH (glyceraldehyde-3-phosphate dehydrogenase protein). All samples were used in duplicate and housekeeping genes were run on the same plate in the iQ-apparatus as the gene of interest. Primer sequences are provided in Table 1C.

WEB RESOURCES

Accession numbers and URLs for data presented in this article are as follows: GenBank, http://ncbi.nlm.nih.gov/GenBank [Accession numbers NT_005612.15, AF_075430, AF_075431, NM_000526, NM_001101, NM_001002 and NM_002046 (these are in Table 1.), AAG45610, AAP87985, CAC37099, BAB20631, AAK15622, AAN03691 (these are in multiple sequence alignment in Fig. 5A].

Online Mendelian Inheritance in Man (OMIM), http://ncbi.nlm.nih.gov/Omim/.

Translation Start Prediction Netstart 1.0, http://www.cbs.dtu.dk/services/NetStart-1.0.

ACKNOWLEDGEMENTS

We thank Dr J. Murray, Dr K. Krahn, Dr S. Daack-Hirsch and Dr A. Mach-Schoenebeck for clinical and diagnostic investigations. We thank Dr B. Andersen and Dr E. Candi for the K14 luciferase construct. And finally we thank all patients for their participation in this study.

Conflict of Interest statement. None declared.

FUNDING

Work in our laboratory is supported by the European Union Sixth Framework programme EpiStem project (LSHB-CT-2005-019067).

REFERENCES

1. Yang, A., Schweitzer, R., Sun, D., Kaghad, M., Walker, N., Bronson, R.T., Tabin, C., Sharpe, A., Caput, D., Crum, C. *et al.* (1999) p63 is essential for regenerative proliferation in limb, craniofacial and epithelial development. *Nature*, **398**, 714–718.
2. Mills, A.A., Zheng, B., Wang, X.J., Vogel, H., Roop, D.R. and Bradley, A. (1999) p63 is a p53 homologue required for limb and epidermal morphogenesis. *Nature*, **398**, 708–713.
3. Yang, A., Walker, N., Bronson, R., Kaghad, M., Oosterwegel, M., Bonnin, J., Vagner, C., Bonnet, H., Dikkes, P., Sharpe, A. *et al.* (2000) p73-deficient mice have neurological, pheromonal and inflammatory defects but lack spontaneous tumours. *Nature*, **404**, 99–103.
4. Sasaki, Y., Ishida, S., Morimoto, I., Yamashita, T., Kojima, T., Kihara, C., Tanaka, T., Imai, K., Nakamura, Y. and Tokino, T. (2002) The p53 family member genes are involved in the Notch signal pathway. *J. Biol. Chem.*, **277**, 719–724.
5. Huang, Y.P., Kim, Y., Li, Z., Fomenkov, T., Fomenkov, A. and Ratovitski, E.A. (2005) AEC-associated p63 mutations lead to alternative splicing/protein stabilization of p63 and modulation of Notch signaling. *Cell Cycle*, **4**, 1440–1447.
6. Barbieri, C.E., Barton, C.E. and Pietenpol, J.A. (2003) Delta Np63 alpha expression is regulated by the phosphoinositide 3-kinase pathway. *J. Biol. Chem.*, **278**, 51408–51414.
7. Caserta, T.M., Kommagani, R., Yuan, Z., Robbins, D.J., Mercer, C.A. and Kadakia, M.P. (2006) p63 overexpression induces the expression of Sonic Hedgehog. *Mol. Cancer Res.*, **4**, 759–768.
8. Laurikkala, J., Mikkola, M.L., James, M., Tummers, M., Mills, A.A. and Thesleff, I. (2006) p63 regulates multiple signalling pathways required for ectodermal organogenesis and differentiation. *Development*, **133**, 1553–1563.
9. Senoo, M., Pinto, F., Crum, C.P. and McKeon, F. (2007) p63 Is essential for the proliferative potential of stem cells in stratified epithelia. *Cell*, **129**, 523–536.
10. Dohn, M., Zhang, S. and Chen, X. (2001) p63alpha and DeltaNp63alpha can induce cell cycle arrest and apoptosis and differentially regulate p53 target genes. *Oncogene*, **20**, 3193–3205.
11. Helton, E.S., Zhu, J. and Chen, X. (2006) The unique NH2-terminally deleted (DeltaN) residues, the PXXP motif, and the PPXY motif are required for the transcriptional activity of the DeltaN variant of p63. *J. Biol. Chem.*, **281**, 2533–2542.
12. Serber, Z., Lai, H.C., Yang, A., Ou, H.D., Sigal, M.S., Kelly, A.E., Darimont, B.D., Duijf, P.H., van, B.H., McKeon, F. *et al.* (2002) A C-terminal inhibitory domain controls the activity of p63 by an intramolecular mechanism. *Mol. Cell Biol.*, **22**, 8601–8611.
13. Celli, J., Duijf, P., Hamel, B.C., Bamshad, M., Kramer, B., Smits, A.P., Newbury-Ecob, R., Hennekam, R.C., Van, B.G., van, H.A. *et al.* (1999) Heterozygous germline mutations in the p53 homolog p63 are the cause of EEC syndrome. *Cell*, **99**, 143–153.
14. van Bokhoven, H., Jung, M., Smits, A.P., van Beersum, S., Ruschendorf, F., van Steensel, M., Veenstra, M., Tuerlings, J.H., Mariman, E.C., Brunner, H.G. *et al.* (1999) Limb mammary syndrome: a new genetic disorder with mammary hypoplasia, ectrodactyly, and other Hand/Foot

anomalies maps to human chromosome 3q27. *Am. J. Hum. Genet.*, **64**, 538–546.
15. Rinne, T., Brunner, H.G. and van, B.H. (2007) p63-associated disorders. *Cell Cycle*, **6**, 262–268.
16. van Bokhoven, H. and Brunner, H.G. (2002) Splitting p63. *Am. J. Hum. Genet.*, **71**, 1–13.
17. Bertola, D.R., Kim, C.A., Albano, L.M., Scheffer, H., Meijer, R. and van, B.H. (2004) Molecular evidence that AEC syndrome and Rapp-Hodgkin syndrome are variable expression of a single genetic disorder. *Clin. Genet.*, **66**, 79–80.
18. McGrath, J.A., Duijf, P.H., Doetsch, V., Irvine, A.D., de, W.R., Vanmolkot, K.R., Wessagowit, V., Kelly, A., Atherton, D.J., Griffiths, W.A. *et al.* (2001) Hay-Wells syndrome is caused by heterozygous missense mutations in the SAM domain of p63. *Hum. Mol. Genet.*, **10**, 221–229.
19. Barrow, L.L., van, B.H., ack-Hirsch, S., Andersen, T., van Beersum, S.E., Gorlin, R. and Murray, J.C. (2002) Analysis of the p63 gene in classical EEC syndrome, related syndromes, and non-syndromic orofacial clefts. *J. Med. Genet.*, **39**, 559–566.
20. Bougeard, G., Hadj-Rabia, S., Faivre, L., Sarafan-Vasseur, N. and Frebourg, T. (2003) The Rapp-Hodgkin syndrome results from mutations of the TP63 gene. *Eur. J. Hum. Genet.*, **11**, 700–704.
21. Dianzani, I., Garelli, E., Gustavsson, P., Carando, A., Gustafsson, B., Dahl, N. and Anneren, G. (2003) Rapp-Hodgkin and AEC syndromes due to a new frameshift mutation in the TP63 gene. *J. Med. Genet.*, **40**, e133.
22. Kantaputra, P.N., Hamada, T., Kumchai, T. and McGrath, J.A. (2003) Heterozygous mutation in the SAM domain of p63 underlies Rapp-Hodgkin ectodermal dysplasia. *J. Dent. Res.*, **82**, 433–437.
23. Tsutsui, K., Asai, Y., Fujimoto, A., Yamamoto, M., Kubo, M. and Hatta, N. (2003) A novel p63 sterile alpha motif (SAM) domain mutation in a Japanese patient with ankyloblepharon, ectodermal defects and cleft lip and palate (AEC) syndrome without ankyloblepharon. *Br. J. Dermatol.*, **149**, 395–399.
24. Chan, I., McGrath, J.A. and Kivirikko, S. (2005) Rapp-Hodgkin syndrome and the tail of p63. *Clin. Exp. Dermatol.*, **30**, 183–186.
25. Payne, A.S., Yan, A.C., Ilyas, E., Li, W., Seykora, J.T., Young, T.L., Pawel, B.R., Honig, P.J., Camacho, J., Imaizumi, S. *et al.* (2005) Two novel TP63 mutations associated with the ankyloblepharon, ectodermal defects, and cleft lip and palate syndrome: a skin fragility phenotype. *Arch. Dermatol.*, **141**, 1567–1573.
26. Shotelersuk, V., Janklat, S., Siriwan, P. and Tongkobpetch, S. (2005) De novo missense mutation, S541Y, in the p63 gene underlying Rapp-Hodgkin ectodermal dysplasia syndrome. *Clin. Exp. Dermatol.*, **30**, 282–285.
27. Kannu, P., Savarirayan, R., Ozoemena, L., White, S.M. and McGrath, J.A. (2006) Rapp-Hodgkin ectodermal dysplasia syndrome: the clinical and molecular overlap with Hay-Wells syndrome. *Am. J. Med. Genet. A*, **140**, 887–891.
28. Rinne, T., Hamel, B., Bokhoven, H. and Brunner, H.G. (2006) Pattern of p63 mutations and their phenotypes-update. *Am. J. Med. Genet. A*, **140**, 1396–1406.
29. Sorasio, L., Ferrero, G.B., Garelli, E., Brunello, G., Martano, C., Carando, A., Belligni, E., Dianzani, I. and Cirillo, S.M. (2006) AEC syndrome: further evidence of a common genetic etiology with Rapp-Hodgkin syndrome. *Eur. J. Med. Genet.*, **49**, 520–522.
30. Fomenkov, A., Huang, Y.P., Topaloglu, O., Brechman, A., Osada, M., Fomenkova, T., Yuriditsky, E., Trink, B., Sidransky, D. and Ratovitski, E. (2003) P63 alpha mutations lead to aberrant splicing of keratinocyte growth factor receptor in the Hay-Wells syndrome. *J. Biol. Chem.*, **278**, 23906–23914.
31. Brunner, H.G., Hamel, B.C. and van, B.H. (2002) The p63 gene in EEC and other syndromes. *J. Med. Genet.*, **39**, 377–381.
32. Maquat, L.E. (1995) When cells stop making sense: effects of nonsense codons on RNA metabolism in vertebrate cells. *RNA*, **1**, 453–465.
33. Kozak, M. (1987) Effects of intercistronic length on the efficiency of reinitiation by eucaryotic ribosomes. *Mol. Cell Biol.*, **7**, 3438–3445.
34. Kozak, M. (1997) Recognition of AUG and alternative initiator codons is augmented by G in position +4 but is not generally affected by the nucleotides in positions +5 and +6. *EMBO J.*, **16**, 2482–2492.
35. Zhang, J. and Maquat, L.E. (1997) Evidence that translation reinitiation abrogates nonsense-mediated mRNA decay in mammalian cells. *EMBO J.*, **16**, 826–833.
36. Perrin-Vidoz, L., Sinilnikova, O.M., Stoppa-Lyonnet, D., Lenoir, G.M. and Mazoyer, S. (2002) The nonsense-mediated mRNA decay pathway triggers degradation of most BRCA1 mRNAs bearing premature termination codons. *Hum. Mol. Genet.*, **11**, 2805–2814.
37. Buisson, M., Anczukow, O., Zetoune, A.B., Ware, M.D. and Mazoyer, S. (2006) The 185delAG mutation (c.68_69delAG) in the BRCA1 gene triggers translation reinitiation at a downstream AUG codon. *Hum. Mutat.*, **27**, 1024–1029.
38. Paulsen, M., Lund, C., Akram, Z., Winther, J.R., Horn, N. and Moller, L.B. (2006) Evidence that translation reinitiation leads to a partially functional Menkes protein containing two copper-binding sites. *Am. J. Hum. Genet.*, **79**, 214–229.
39. Puel, A., Reichenbach, J., Bustamante, J., Ku, C.L., Feinberg, J., Doffinger, R., Bonnet, M., Filipe-Santos, O., Beaucoudrey, L., Durandy, A. *et al.* (2006) The NEMO mutation creating the most-upstream premature stop codon is hypomorphic because of a reinitiation of translation. *Am. J. Hum. Genet.*, **78**, 691–701.
40. Candi, E., Rufini, A., Terrinoni, A., Dinsdale, D., Ranalli, M., Paradisi, A., De, L.V., Spagnoli, L.G., Catani, M.V., Ramadan, S. *et al.* (2006) Differential roles of p63 isoforms in epidermal development: selective genetic complementation in p63 null mice. *Cell Death Differ.*, **13**, 1037–1047.
41. Romano, R.A., Birkaya, B. and Sinha, S. (2007) A functional enhancer of keratin14 is a direct transcriptional target of deltaNp63. *J. Invest Dermatol.*, **127**, 1175–1186.
42. Ortt, K. and Sinha, S. (2006) Derivation of the consensus DNA-binding sequence for p63 reveals unique requirements that are distinct from p53. *FEBS Lett.*, **580**, 4544–4550.
43. Yang, A., Kaghad, M., Wang, Y., Gillett, E., Fleming, M.D., Dotsch, V., Andrews, N.C., Caput, D. and McKeon, F. (1998) p63, a p53 homolog at 3q27-29, encodes multiple products with transactivating, death-inducing, and dominant-negative activities. *Mol. Cell*, **2**, 305–316.
44. King, K.E., Ponnamperuma, R.M., Yamashita, T., Tokino, T., Lee, L.A., Young, M.F. and Weinberg, W.C. (2003) deltaNp63alpha functions as both a positive and a negative transcriptional regulator and blocks in vitro differentiation of murine keratinocytes. *Oncogene*, **22**, 3635–3644.
45. Yang, A., Zhu, Z., Kapranov, P., McKeon, F., Church, G.M., Gingeras, T.R. and Struhl, K. (2006) Relationships between p63 binding, DNA sequence, transcription activity, and biological function in human cells. *Mol. Cell*, **24**, 593–602.
46. Chen, C.A. and Okayama, H. (1988) Calcium phosphate-mediated gene transfer: a highly efficient transfection system for stably transforming cells with plasmid DNA. *Biotechniques*, **6**, 632–638.
47. de Brouwer, A.P., Williams, K.L., Duley, J.A., van Kuilenburg, A.B., Nabuurs, S.B., Egmont-Petersen, M., Lugtenberg, D., Zoetekouw, L., Banning, M.J., Roeffen, M. *et al.* (2007) Arts syndrome is caused by loss-of-function mutations in PRPS1. *Am. J. Hum. Genet.*, **81**, 507–518.
48. Livak, K.J. and Schmittgen, T.D. (2001) Analysis of relative gene expression data using real-time qPCR and the 2(-Delta Delta C(T)) Method. *Methods*, **25**, 402–408.
49. Pfaffl, M.W. (2001) A new mathematical model for relative quantification in real-time RT-PCR. *Nucleic Acids Res.*, **29**, e45.